ORIGINAL ARTICLE

Cancer Science WILEY

Akt inhibition synergizes with polycomb repressive complex 2 inhibition in the treatment of multiple myeloma

Mohamed Rizk[1,2] [iD] | Ola Rizq[1,3] | Motohiko Oshima[1,2] | Yaeko Nakajima-Takagi[1,2] | Shuhei Koide[2] | Atsunori Saraya[1] | Yusuke Isshiki[1,4,5] | Tetsuhiro Chiba[6] | Satoshi Yamazaki[7] | Anqi Ma[8,9] | Jian Jin[8,9] | Atsushi Iwama[1,2] | Naoya Mimura[10]

[1]Department of Cellular and Molecular Medicine, Graduate School of Medicine, Chiba University, Chiba, Japan

[2]Division of Stem Cell and Molecular Medicine, Center for Stem Cell Biology and Regenerative Medicine, The Institute of Medical Science, The University of Tokyo, Tokyo, Japan

[3]Department of Medical Oncology, LeBow Institute for Myeloma Therapeutics and Jerome Lipper Multiple Myeloma Center, Dana-Farber Cancer Institute, Harvard Medical School, Boston, MA, USA

[4]Department of Hematology, Chiba University Hospital, Chiba, Japan

[5]Department of Clinical Cell Biology and Medicine, Graduate School of Medicine, Chiba University, Chiba, Japan

[6]Department of Gastroenterology, Graduate School of Medicine, Chiba University, Chiba, Japan

[7]Division of Stem Cell Biology, Center for Stem Cell Biology and Regenerative Medicine, The Institute of Medical Science, The University of Tokyo, Tokyo, Japan

[8]Department of Pharmacological Sciences, Mount Sinai Center for Therapeutics Discovery, Tisch Cancer Institute, Icahn School of Medicine at Mount Sinai, New York, NY, USA

[9]Department of Oncological Sciences, Mount Sinai Center for Therapeutics Discovery, Tisch Cancer Institute, Icahn School of Medicine at Mount Sinai, New York, NY, USA

[10]Department of Transfusion Medicine and Cell Therapy, Chiba University Hospital, Chiba, Japan

Correspondence
Atsushi Iwama, Division of Stem Cell and Molecular Medicine, Center for Stem Cell Biology and Regenerative Medicine, The Institute of Medical Science, The University of Tokyo, 4-6-1 Shirokanedai, Minato-ku, Tokyo 108-8639, Japan.
Email: 03aiwama@ims.u-tokyo.ac.jp

Naoya Mimura, Department of Transfusion Medicine and Cell Therapy, Chiba University Hospital, 1-8-1 Inohana, Chuo-ku, Chiba 260-8677, Japan.
Email: naoyamimura@chiba-u.jp

Abstract

Polycomb repressive complex 2 (PRC2) components, EZH2 and its homolog EZH1, and PI3K/Akt signaling pathway are focal points as therapeutic targets for multiple myeloma. However, the exact crosstalk between their downstream targets remains unclear. We herein elucidated some epigenetic interactions following Akt inhibition and demonstrated the efficacy of the combined inhibition of Akt and PRC2. We found that TAS-117, a potent and selective Akt inhibitor, downregulated EZH2 expression at the mRNA and protein levels via interference with the Rb-E2F pathway, while EZH1 was compensatively upregulated to maintain H3K27me3 modifications. Consistent with these results, the dual EZH2/EZH1 inhibitor, UNC1999, but not the selective EZH2 inhibitor, GSK126, synergistically enhanced TAS-117-induced cytotoxicity and provoked myeloma cell apoptosis. RNA-seq analysis revealed the activation of the FOXO signaling pathway after TAS-117 treatment. *FOXO3/4* mRNA and their downstream targets were upregulated with the enhanced nuclear localization of FOXO3 protein after TAS-117 treatment. ChIP assays confirmed the direct binding of FOXO3 to *EZH1* promoter, which was enhanced by TAS-117 treatment. Moreover, *FOXO3*

knowdown repressed *EZH1* expression. Collectively, the present results reveal some molecular interactions between Akt signaling and epigenetic modulators, which emphasize the benefits of targeting PRC2 full activity and the Akt pathway as a therapeutic option for multiple myeloma.

1 | INTRODUCTION

Multiple myeloma (MM), the second most common hematological malignancy, is an incurable and fatal disease that eventually recurs as a result of intrinsic and/or acquired drug resistance despite recent therapeutic advances.[1,2] MM is characterized by the close relationship between malignant plasma cells and stromal and endothelial cells in the bone marrow microenvironment, which secrete growth factors, such as interleukin-6 (IL-6) and insulin-like growth factor 1 (IGF1), thereby stimulating survival pathways, including MEK/ERK, JAK/STAT and PI3K/Akt, which promote myeloma cell growth, survival and drug resistance, respectively.[2-4] The PI3K/Akt pathway is constitutively activated in a significant proportion of myeloma patients[3]; despite the paucity of activating mutations in the pathway downstream effectors, or inactivating mutations in the tumor suppressor *PTEN*.[5,6] PI3K/Akt targets multiple downstream effectors by activating and inactivating phosphorylation of, for example, mTORC1 and FOXO transcription factors (TFs), respectively, thereby maintaining cell proliferation and survival.[7] A plethora of studies have extensively investigated Akt inhibitors, alone or in combination, in multiple phase I and II clinical trials; however, the outcomes in hematological malignancies have been largely unsatisfactory,[8] emphasizing the need for critical preclinical evaluations of Akt inhibitors in combination with other targeted therapies.[9] TAS-117, a potent and selective non-competitive Akt inhibitor against MM,[10] is currently in ongoing phase II clinical trials against solid tumors (https://www.clinicaltrials.jp/cti-user/common/Top.jsp JapicCTI-152780). However, its preclinical evaluation in hematological malignancies warrants further research to achieve optimum combination outcomes.

Polycomb repressive complex 2 (PRC2) is an epigenetic modulator that tri-methylates histone H3 at lysine 27 (H3K27me3) through its catalytic components (enhancer of zeste 2 (EZH2) and its closely related homolog EZH1) to silence the transcription of its target genes.[11] *EZH2* is aberrantly overexpressed or subjected to gain-of-function mutations in various malignant tumors,[12] including hematological malignancies.[13,14] In MM, *EZH2* is overexpressed and correlates not only with the development of asymptomatic monoclonal gammopathy of undetermined significance (MGUS) to active full-blown myeloma[13,15] but also with disease prognosis and poor survival,[16] which emphasizes the importance of targeting EZH2 in the treatment of MM. Preclinical investigations on "selective" EZH2 inhibitors involved some of them in clinical trials against various

tumors, including MM.[12] However, neither the compensatory role of EZH1[17,18] nor its complementary effects on the action of EZH2[19-21] can be ignored. Moreover, the inhibition of EZH2 alone was not sufficient to completely disrupt the oncogenic functions of PRC2 in different malignancies, including acute myeloid leukemia[21] and MM,[19,20] pointing to the benefit of targeting both EZH2 and EZH1 in PRC2-dependent cancers.

The interplay between signaling cascades and epigenetic modulators is poorly understood in MM. The majority of signal transduction pathways need to eventually be translated into specific transcriptional signatures, which, in part, are achieved through the modulation of chromatin modifiers, including PRC2 components, thereby enhancing or repressing transcription at specific loci. Although some of these interactions have been described in solid tumors,[22-24] limited information is currently available on this crosstalk in hematological malignancies, including MM. Given the importance of PRC2 as a therapeutic target in MM, we aimed to investigate the mechanisms by which Akt inhibition may impact PRC2 function and highlight whether targeting both EZH2 and EZH1 together with Akt inhibition is a promising treatment strategy for MM.

2 | MATERIALS AND METHODS

2.1 | Reagents

TAS-117, trans-3-amino-1methyl-3-[4-(3-phenyl-5H-imidazo [1,2-c] pyrido[3,4-e][1,3]oxazin-2-yl)phenyl]-cyclobutanol, was obtained from Taiho Pharmaceutical Co., Ltd. and diluted in DMSO to form a stock of 20 µmol/L. UNC1999 was produced at the Icahn School of Medicine at Mount Sinai[25] and was diluted in DMSO to a stock of 10 mmol/L. GSK126 was purchased from CHEMIETEK and was diluted in DMSO to a stock of 20 mmol/L.

2.2 | RNA-seq library construction and sequencing analysis

The MM cell lines, MM.1S and H929, were treated with or without TAS-117 (0.5 µmol/L) for 24 hours. Total RNA was extracted using an RNeasy Plus Micro Kit (Qiagen). RNA concentrations and integrity were verified using Agilent 2100 Bioanalyzer. cDNA libraries were generated using a NEBNext Ultra RNA Library Prep Kit (New

England BioLabs). Sequencing was performed using HiSeq1500 (Illumina) with a single-read sequencing length of 60 bp. TopHat (version 2.0.13; with default parameters) was used for mapping to the reference genome (UCSC/hg19) from the University of California, Santa Cruz Genome Browser (http://genome.ucsc.edu/) with annotation data from iGenomes (Illumina). Levels of gene expression were then quantified as reads per kilobase of exon unit per million mapped reads (RPKM) using Cuffdiff (Cufflinks version 2.2.1; with default parameters). Overexpressed genes (>1.5-fold) in both MM.1S and H929 cells, after TAS-117 treatment, are listed in Table S1.

2.3 | Gene ontology analysis

Lists of overexpressed genes after the TAS-117 treatment (>1.5-fold enrichment, shown in Table S1) were analyzed for gene ontology with DAVID resources (database used for annotation, visualization and integrated discovery) (http://david.abcc.ncifcrf.gov).

2.4 | ChIP assays

In FOXO3 ChIP experiments, MM.1S and H929 cells (40×10^6) were incubated with TAS-117 (0.5 μmol/L) for 48 hours. Cells were harvested and washed with ice-cold PBS. DNA and proteins were crosslinked by the addition of paraformaldehyde (PFA) to a final concentration of 1% at 25°C for 10 minutes. Cells were centrifuged, lysed in RIPA buffer (50 mmol/L Tris-HCl, pH 8.0, 150 mmol/L NaCl, 2 mmol/L EDTA, pH 8.0, 1% NP-40 substitute, 0.5% sodium deoxycholate and 0.1% SDS) supplemented with protease inhibitor cocktail (Roche), and then sonicated (ultrasonic homogenizer, MICROTEC). The soluble chromatin fraction was recovered, pre–cleared with sheep anti–mouse IgG Dynabeads (Thermo Fisher), and then immunoprecipitated at 4°C overnight with 5 μg anti–FOXO3 (clone D12: sc-48348X, Santa Cruz). Immunoprecipitates were thoroughly washed. DNA was purified using the MinElute PCR purification kit (Qiagen). In the ChIP assay, quantitative PCR (qPCR) was performed with the Step One Plus real-time PCR system using SYBR Premix ExTaq II (Tli RNase Plus) from Takara. Primers for the *EZH1* promoter regions, the FOXO3-positive locus (*BIM*)[26] and the FOXO3-negative locus (*GAPDH*),[27] are listed in Table S2.

2.5 | Statistical analysis

The significance of differences was measured using an unpaired two-tailed Student's *t* test or Welch's test, if unequal variances were examined. Tests were calculated using GraphPad Prism, version 7. Data are shown as the mean ± SD. Significance was taken at values of *P < 0.05, **P < 0.01 and ***P < 0.001. The combined effect of UNC1999 or GSK126 with TAS-117 was analyzed by isobologram analysis using the CompuSyn software program to calculate the combination index (CI) (Table S3) for each combination (ComboSyn, Inc[28]).

Detailed methods for cell lines and cultures, cytotoxicity assay, immunoblot and immunofluorescence analyses, quantitative reverse

transcription PCR (RT-PCR), assays of apoptosis, and lentiviral vectors are detailed in the Supplementary Methods section.

2.6 | Deposition of data

RNA sequence data were deposited in the DNA Data Bank of Japan (DDBJ) (accession number: DRA008478).

3 | RESULTS

3.1 | UNC1999 enhances TAS-117-induced cytotoxicity in multiple myeloma cells

We incubated a subset of MM cell lines with increasing concentrations of TAS-117 for 48 hours to evaluate the cytotoxic effects of Akt inhibition. Seven cell lines with different genetic backgrounds were used. We found heterogeneity in the responsiveness of MM cell lines to Akt inhibition. TAS-117 induced significant cytotoxicity in MM.1S, H929 and OPM2/BTZ cell lines (Figure 1A). We then examined whether a relationship exists between the sensitivity to Akt inhibition and the intrinsic levels of activated phospho-Akt (p-Akt). In accordance with previous findings,[10,29,30] TAS-117-sensitive cell lines had high levels of activated Akt, phosphorylated at serine 473 (p-Akt-ser473) (Figure 1B), suggesting their dependency on the Akt pathway as a pro–survival stimulant. The high p-Akt baseline correlated with sensitivity to Akt inhibition, except in KMS11 cell line, which had activated Akt with no sensitivity to TAS-117 treatment. However, phosphorylation levels at threonine 308 (thr308), which weakly activate Akt, did not correlate with TAS-117 sensitivity (Figure 1B). Of note, cells with high p-Akt-ser levels showed markedly lower levels of the tumor suppressor, *PTEN*, than cell lines with low p-Akt-ser levels (Figure S1A), suggesting an inverse relationship between the responsiveness to the Akt inhibitor and the intrinsic level of *PTEN*. The bortezomib-resistant cell line OPM2/BTZ, generated from parental OPM2 cells,[31] had the highest p-Akt levels, which were associated with the lack of *PTEN* expression (Figure 1B and Figure S1A).

Crosstalk between epigenetic modulators and signaling pathways has already been reported in some contexts.[14,22-24] Bisserier and Wajapeyee (2018) found that resistance to EZH2 inhibition in lymphoma cells may be acquired through the activation of the PI3K/Akt pathway, and the inhibition of PI3K sensitized resistant cancer cells to the cytotoxic effects of EZH2 inhibitors.[32] Based on these findings, we treated myeloma cell lines with TAS-117 in combination with either the dual EZH2/EZH1 inhibitor, UNC1999 (IC50, EZH2 < 10 nmol/L; EZH1 45 nmol/L),[33] or a selective EZH2 inhibitor, GSK126 (IC50, EZH2 9.9 nmol/L; EZH1 680 nmol/L).[34] Interestingly, dual EZH2/EZH1 inhibition using UNC1999 enhanced the cytotoxicity induced by TAS-117 more effectively than the selective EZH2 inhibitor, GSK126 (Figure 1C,D and Figure S1B). The combination outcome was validated using CompuSyn software,[35] calculating the CI. The analysis confirmed the synergism between UNC1999 and TAS-117, achieving CI that was markedly lower than 1, in MM.1S (Figure 1C "right panels" and Table S3A). In addition, in H929 and

(A)

(B)

(C) MM.1S

MM.1S

(D) H929

H929

(E)
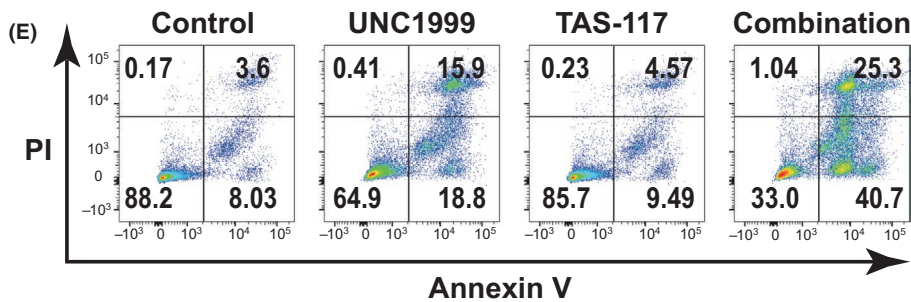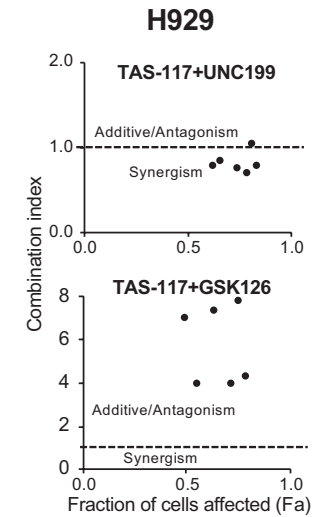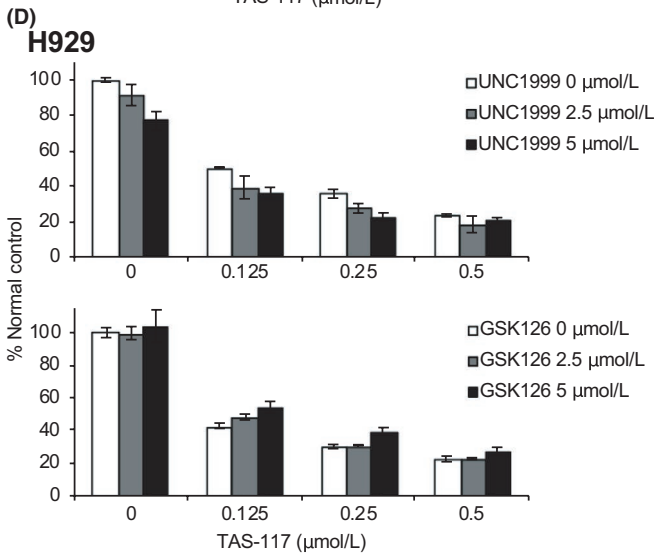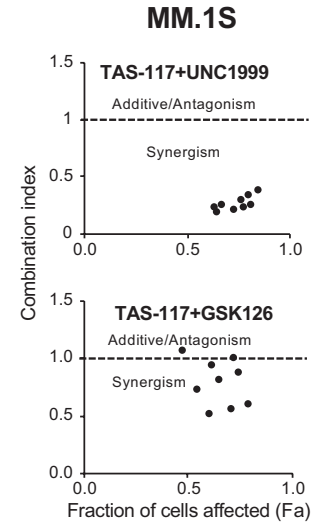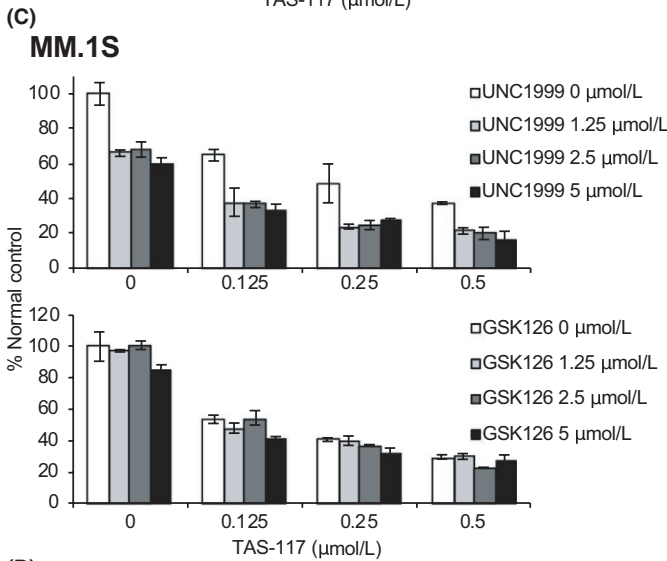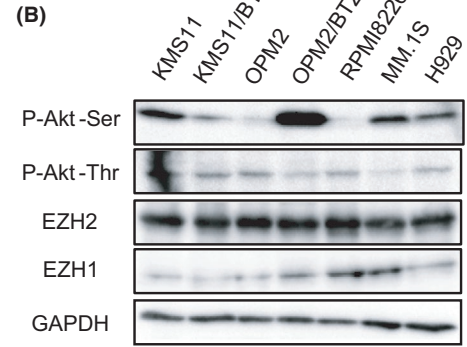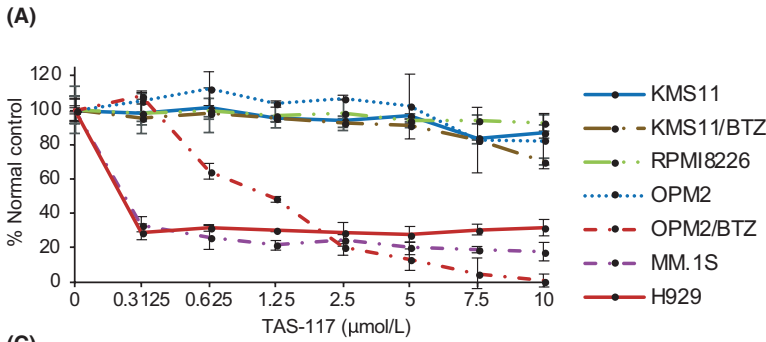
FIGURE 1 UNC1999 enhances TAS-117-induced cytotoxicity in multiple myeloma (MM) cells. A, KMS11, KMS11/BTZ, RPMI8226, OPM2, OPM2/BTZ, MM.1S and H929 cells were treated with the indicated concentrations of TAS-117, up to 10 μmol/L, for 48 h and the percentage of cell viability was assessed by the MTS assay relative to an untreated control. Data represent the mean ± SD of triplicates. B, Immunoblots for the basal expression of the indicated antibodies in the cell lines used in (A). GAPDH served as the loading control. C and D, MTS assay showing the viability of MM.1S (C) or H929 cells (D) after treatment with the indicated doses of UNC1999 "upper panels" or GSK126 "lower panels" for 72 h in combination with the indicated doses of TAS-117 for the last 48 h, relative to the untreated control. Data represent the mean ± SD of triplicates. The calculation of the combination index for each combination is shown to the right of each graph. E, Flow cytometric analysis, using annexin V/PI staining, for MM.1S cells treated for 48 h with UNC1999 (5 μmol/L) and/or TAS-117 (2 μmol/L) for the last 12 h

OPM2/BTZ cells, CI values for UNC1999 combination was synergistic (<1) and comparatively lower than GSK126 combination values (Figure 1D, Figure S1B "right panels" and Table S3B,C). These results emphasize a crucial role for EZH1 inhibition besides EZH2 inhibition in MM. Of note, TAS-117/UNC1999 combination was effective against TAS-117-sensitive cell lines, while TAS-117-resistant cell lines, such as OPM2 parent cells, showed no synergistic effect (Figure S1C and Table S3D). In an attempt to elucidate the mechanisms by which UNC1999 enhanced TAS-117-induced cytotoxicity in MM cells, we performed a flow cytometric analysis using annexin V/PI staining for single and combined treatments. We found that TAS-117/UNC1999 combination increased the percentage of the annexin V-positive apoptotic cell fraction more than UNC1999 or TAS-117 alone (Figure 1E and Figure S1D). Collectively, these results suggest that TAS-117 inhibits the growth of myeloma cells and that dual EZH2/EZH1 inhibition synergizes with Akt inhibition through the induction of apoptosis.

3.2 | TAS-117 downregulates *EZH2* expression via E2F1 inactivation

Previous studies have reported that *EZH2* expression may, context-dependently, be regulated by different signaling pathways.[14,22-24] Therefore, we examined EZH2 mRNA and protein expression levels in MM.1S, H929 and OPM2/BTZ cell lines when Akt signaling was inhibited. TAS-117 significantly downregulated EZH2 mRNA and its protein levels in the three responsive cell lines in concentration-dependent (Figure 2A,B and Figure S2A) and time-dependent manners (Figure 2C and Figure S2B), while H3K27me3 levels were maintained or elevated, suggesting a possible compensatory effect by EZH1 (Figure 2B,C). Moreover, *EZH2* mRNA levels were additively abolished after the combination of TAS-117 and UNC1999 (Figure 2D). However, *EZH2* expression in the OPM2 parental cell line was not affected by TAS-117 treatment, unlike the bortezomib-resistant cell line (OPM2/BTZ) (Figure S2C,D). Of note, while TAS-117 significantly abolished p-Akt levels (Figure 2B,C and Figure S2A), it resulted in the feedback activation of the MAPK pathway, depicted by the upregulation of p-ERK1/2 and phosphorylation of the PI3K regulatory subunit, p85 (Figure S2E).

To elucidate the mechanisms underlying *EZH2* downregulation, we focused on the retinoblastoma-E2F (Rb-E2F) complex, which transcriptionally regulates many proliferative pathways, including

EZH2.[19,36,37] We previously showed that E2F1 bound to the *EZH2* promoter and activated its expression in myeloma cells, and also that bortezomib treatment downregulated *EZH2* expression by abrogating *E2F1* expression.[19] In the present study, TAS-117 treatment induced marked downregulation of *E2F1* and *E2F2* mRNA and E2F1 protein expression (Figure 2E,F and Figure S2F,G). To further clarify the mechanisms responsible for the *E2F1/2* downregulation/inactivation, we examined the levels of cyclins and cyclin-dependent kinases (CDK), as these are direct targets of the PI3K/Akt cascade and, thus, regulate the phosphorylation of Rb and subsequent destabilization of the Rb-E2F complex.[38] We found that TAS-117 abrogated cyclin D1, CDK1, CDK2 and phospho-Rb levels with the marked upregulation of p27 (also known as CDKN1B) (Figure 2F and Figure S2G). Collectively, these results confirm that inhibition of the Akt cascade regulates the expression of *EZH2* through the interaction/stabilization of the Rb-E2F complex.

3.3 | EZH1 compensates for the downregulation of EZH2 by Akt inhibition

Previous studies have suggested that EZH1 augments and complements EZH2 activity and partially compensates for its loss in different contexts.[17,18,20,21,39] We herein demonstrated that H3K27me3 levels were maintained or elevated after TAS-117 treatment (see the data in Figure 2B,C). This result prompted us to hypothesize that the function of EZH1 was augmented following Akt inhibition. RT-qPCR and western blot analyses both confirmed that EZH1 was markedly upregulated after TAS-117 treatment in time-dependent and concentration-dependent manners (Figure 3A-C and Figure S3A-C) in the sensitive cell lines, unlike the TAS-117-resistant parental OPM2 cells (Figure S3D).

Because *EZH1* was markedly upregulated after the inhibition of Akt, and EZH2 and EZH1 both complement each other for chromatin compaction and, hence, transcriptional silencing,[17,18] we hypothesized that the depletion of *EZH1* may enhance the sensitivity of myeloma cells to Akt inhibition. To this end, we transduced MM.1S and H929 with lentiviral shRNA against *EZH1*, which markedly abrogated EZH1 mRNA and protein expression (Figure 4A "left panel" and B) without the compensatory upregulation of *EZH2* (Figure 4A "right panel"). Of note, the *EZH1* level remained normal after *EZH2* knockdown (Figure S3E,F). Importantly, *EZH1* knockdown significantly enhanced the sensitivity of myeloma cells to TAS-117-induced

(A)

(B)

(C)

(D)

(E)

(F)
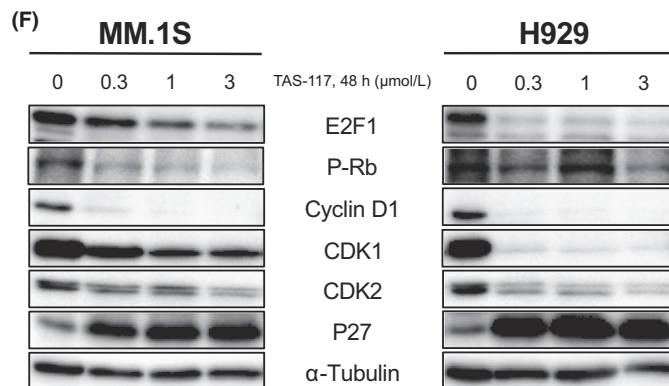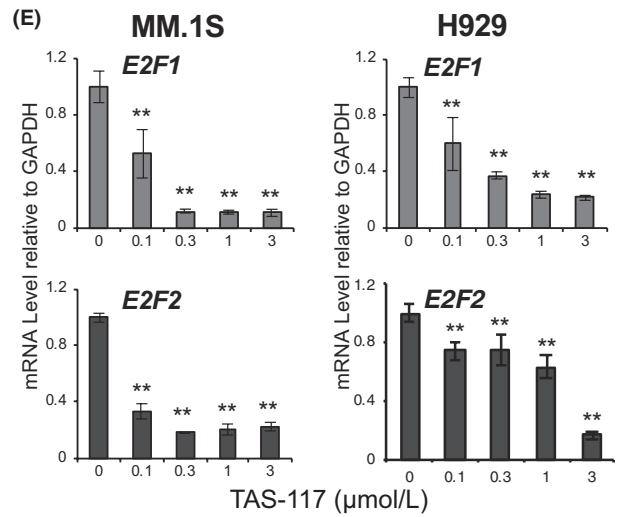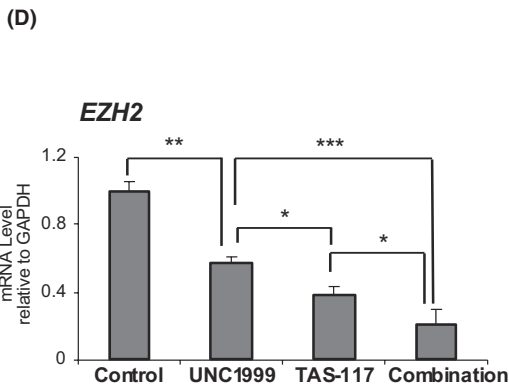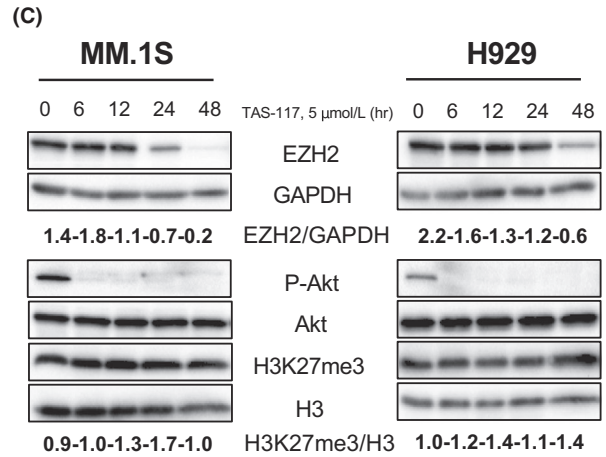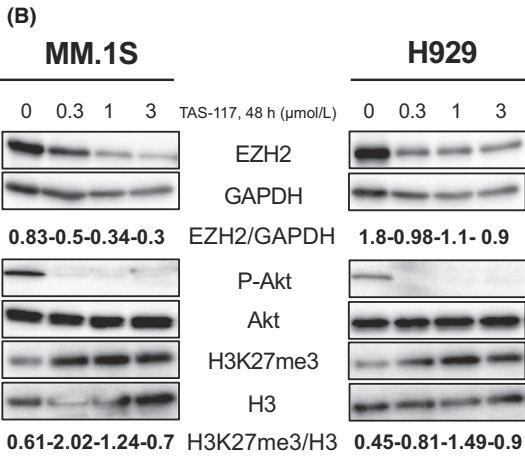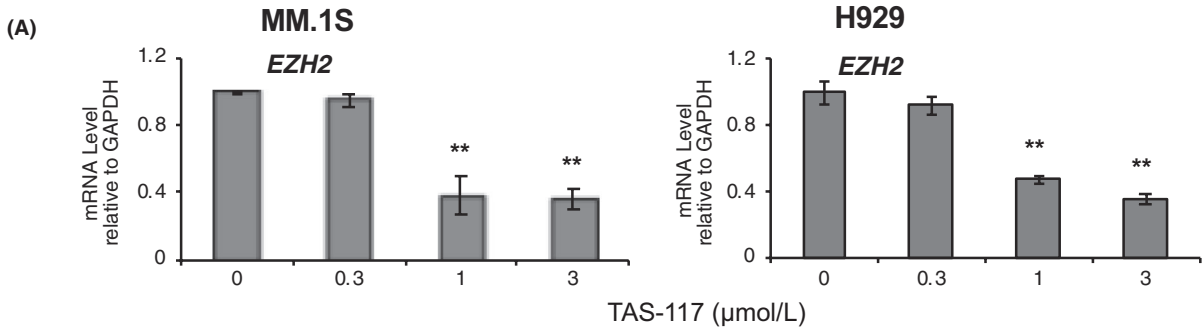
FIGURE 2 TAS-117 downregulates *EZH2* expression via E2F1 inactivation. A, Quantitative RT-PCR analysis for *EZH2* mRNA expression in MM.1S "left panel" and H929 "right panel" cells treated with the indicated doses of TAS-117 for 24 h. The y-axis represents fold changes after the normalization to *GAPDH*, and error bars represent the SD of triplicates. Significance is indicated relative to the untreated control. The list for sequences of primers used for RT-qPCR is described in Table S4. B and C, Immunoblots for the indicated proteins in MM.1S and H929 cells treated with the indicated doses of TAS-117 for 48 h (B) or 5 µmol/L of TAS-117 for the indicated times (C). GAPDH, Akt and H3 served as loading controls. EZH2 and H3K27me3 amounts relative to GAPDH and H3, respectively, are shown. D, Quantitative RT-PCR analysis for *EZH2* mRNA expression in MM.1S cells treated for 72 h with UNC1999 (5 µmol/L) and/or TAS-117 (2 µmol/L) for the last 24 h. The y-axis represents fold changes after the normalization to *GAPDH*, and error bars represent the SD of triplicates. Significance is indicated relative to the compared groups. E, Quantitative RT-PCR analysis for *E2F1* (upper panel) and *E2F2* (lower panel) mRNA expression in MM.1S "left panel" and H929 "right panel" cells treated with the indicated doses of TAS-117 for 24 h. The y-axis represents fold changes after the normalization to *GAPDH*, and error bars represent the SD of triplicates. Significance is indicated relative to the untreated control. F, Immunoblots for the indicated proteins in MM.1S (left) and H929 (right) cells treated with the indicated doses of TAS-117 for 48 h. α-Tubulin served as the loading control. *$P < 0.05$; **$P < 0.01$; ***$P < 0.001$ by Student's t test
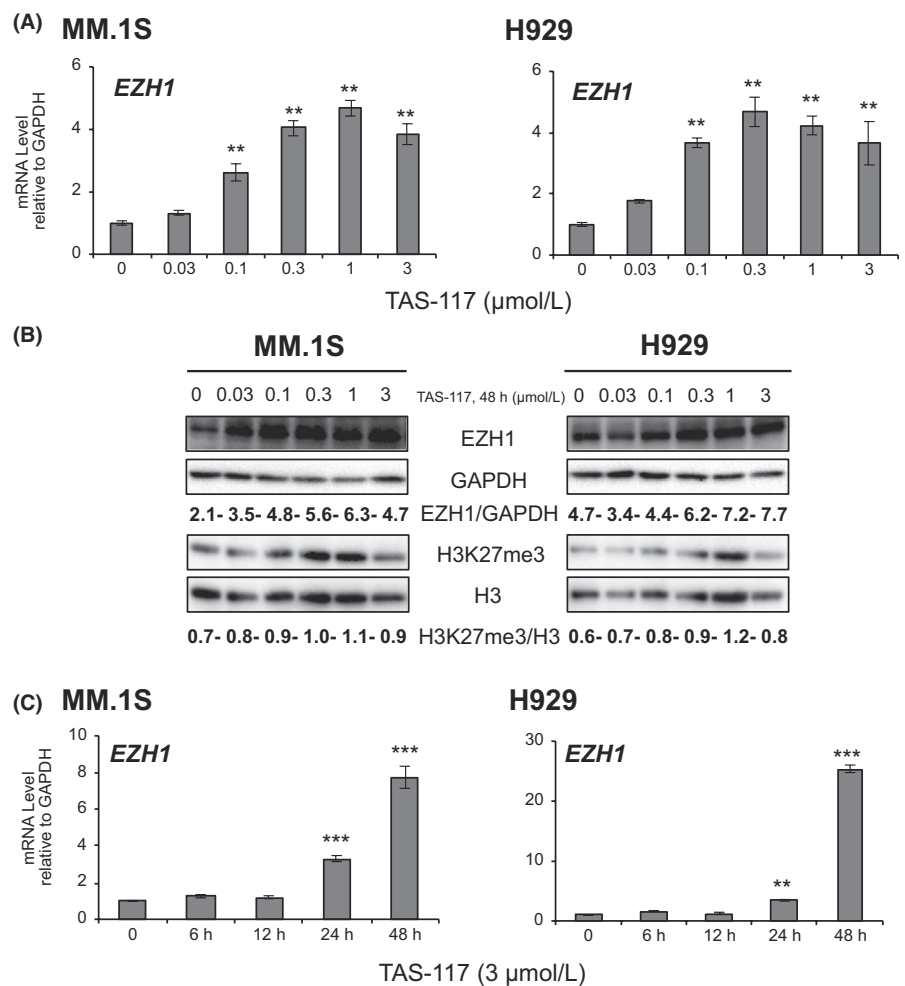
cytotoxicity (Figure 4C). As shown in Figure 2B, H3K27me3 levels were maintained or elevated after TAS-117 treatment. This prompted us to investigate the changes in H3K27me3 levels in *shEZH1*-transduced cells after TAS-117 treatment. To achieve this, *EZH1*-knockdown MM.1S cells were treated with TAS-117 at a lower concentration, as cells became more sensitive to Akt inhibition. We found that H3K27me3 levels after TAS-117 treatment were lower in *EZH1* knockdown cells than in *shLuc*-transduced control cells (Figure 4D), coupled with the attenuated upregulation of *EZH1* mRNA from that in *shLuc* cells (Figure 4E), and the expected downregulation
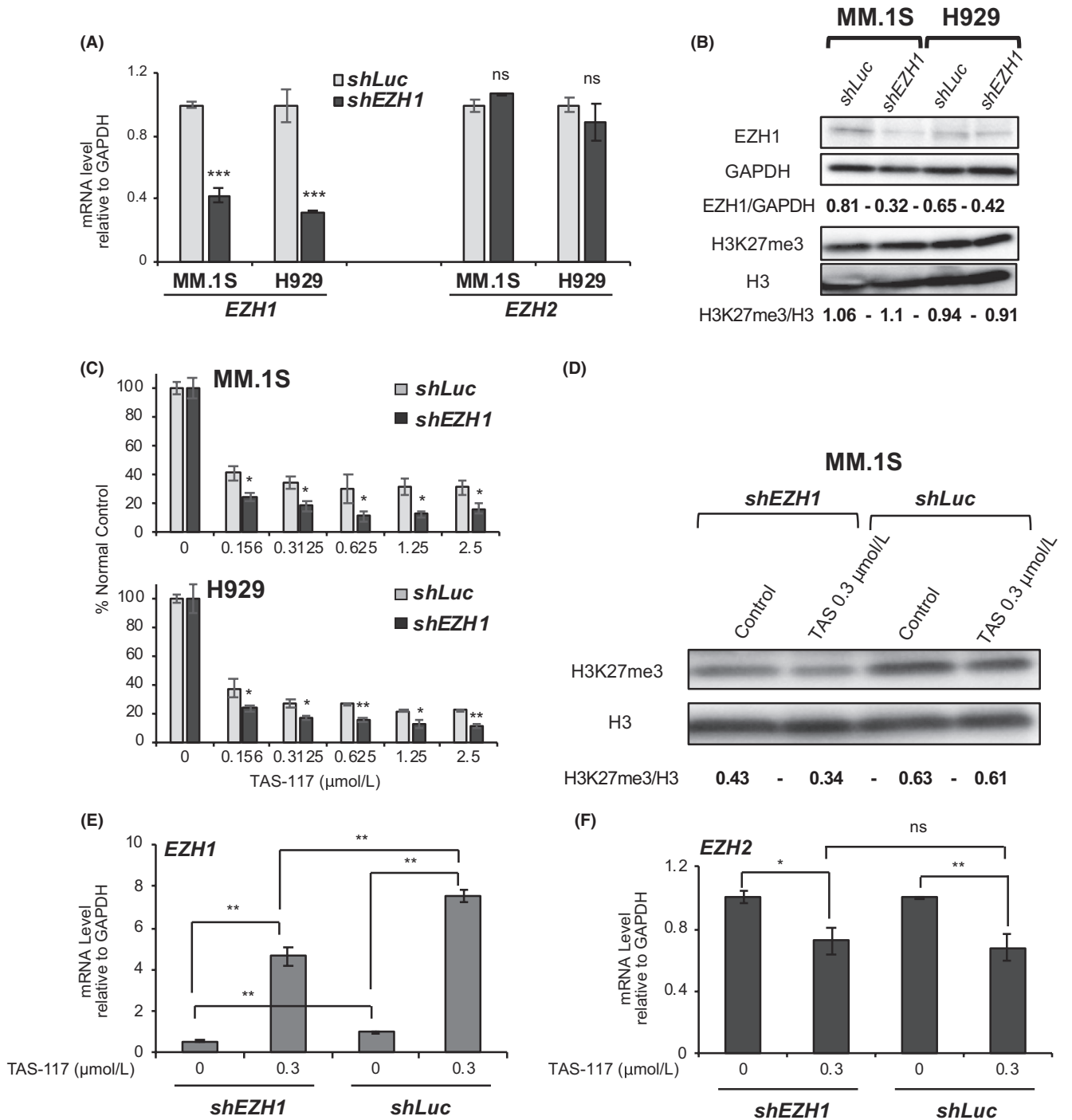
of *EZH2* mRNA (Figure 4F). Collectively, these results indicate that *EZH1* compensates for the downregulation of *EZH2* induced by Akt inhibition and the loss of *EZH1* expression sensitizes MM cells to Akt inhibition.

3.4 | FOXO3 regulates *EZH1* promoter in response to TAS-117 treatment

To clarify the molecular mechanisms underlying *EZH1* upregulation after TAS-117 treatment in myeloma cells, we performed RNA

FIGURE 3 EZH1 compensates for the downregulation of EZH2 by Akt inhibition. A, Quantitative RT-PCR analysis for *EZH1* mRNA expression in MM.1S "left panel" and H929 "right panel" cells treated with the indicated doses of TAS-117 for 24 h. The y-axis represents fold changes after the normalization to *GAPDH*, and error bars represent the SD of triplicates. Significance is indicated relative to the untreated control. B, Immunoblots for the indicated proteins in MM.1S and H929 cells treated with the indicated doses of TAS-117 for 48 h. GAPDH and H3 served as loading controls. EZH1 and H3K27me3 amounts relative to GAPDH and H3, respectively, are shown. C, Quantitative RT-PCR analysis for *EZH1* mRNA expression in MM.1S and H929 cells treated with TAS-117 3 µmol/L for the indicated times. The y-axis represents fold changes after the normalization to *GAPDH*, and error bars represent the SD of triplicates. Significance is indicated relative to the untreated control. **$P < 0.01$; ***$P < 0.001$ by Student's t test

(A) MM.1S / H929 — EZH1 mRNA Level relative to GAPDH, TAS-117 (µmol/L)

(B) MM.1S / H929 immunoblots — TAS-117, 48 h (µmol/L) 0 0.03 0.1 0.3 1 3; EZH1, GAPDH; EZH1/GAPDH MM.1S: 2.1- 3.5- 4.8- 5.6- 6.3- 4.7; H929: 4.7- 3.4- 4.4- 6.2- 7.2- 7.7; H3K27me3, H3; H3K27me3/H3 MM.1S: 0.7- 0.8- 0.9- 1.0- 1.1- 0.9; H929: 0.6- 0.7- 0.8- 0.9- 1.2- 0.8

(C) MM.1S / H929 — EZH1 mRNA Level relative to GAPDH, TAS-117 (3 µmol/L)

FIGURE 4 *EZH1* knockdown sensitizes multiple myeloma (MM) cells to Akt inhibition. A, Quantitative RT-PCR analysis for *EZH1* (left) and *EZH2* (right) mRNA expression in MM.1S and H929 cells transduced with shRNA lentiviral vectors against *EZH1* and luciferase. The y-axis represents fold changes after the normalization to *GAPDH*, and error bars represent the SD of triplicates. Significance is indicated relative to the untreated control. B, Immunoblots for EZH1 and H3K27me3 in MM.1S and H929 cells transduced with shRNA lentiviral vectors against *EZH1* and luciferase. GAPDH and H3 served as loading controls. C, MTS assay showing the viability of MM.1S "left" or H929 "right" cells transduced with shRNA lentiviral vectors against *EZH1* and luciferase and treated with the indicated doses of TAS-117 for 48 h, relative to the untreated control. Data represent the mean ± SD of triplicates. Significance is indicated relative to *shLuc*. D, Immunoblots for H3K27me3 in MM.1S cells transduced with shRNA lentiviral vectors against EZH1 and luciferase and treated with the indicated doses of TAS-117 for 48 h. H3 served as the loading control. E and F, Quantitative RT-PCR analysis for *EZH1* (E) and *EZH2* (F) mRNA expression in MM.1S cells transduced with shRNA lentiviral vectors against *EZH1* and luciferase and treated with the indicated doses of TAS-117 for 24 h. The y-axis represents fold changes after the normalization to *GAPDH*, and error bars represent the SD of triplicates. All groups were normalized to *shLuc*-untreated group. Significance is indicated relative to the compared groups. *$P < 0.05$; **$P < 0.01$; ***$P < 0.001$; ns, not significant by Student's *t* test

sequencing for MM.1S and H929 cells treated with 0.5 μmol/L of TAS-117 for 24 hours. We conducted KEGG pathway analysis (using DAVID bioinformatics database)[40] on genes that were upregulated (>1.5-fold) from those in untreated control cells (Figure 5A and Figure S4A) (1281 genes in MM.1S and 1145 genes in H929, (Table S1)). Among significantly enriched pathways, such as MAPK and NF-κB pathways, FOXO signaling pathway showed the highest enrichment (*P*-value < 2.1^{-08}) (Figure 5A and Figure S4A). We focused on the FOXO pathway as it is a crucial target in MM treatment using PI3K/Akt pathway inhibitors.[41] RT-qPCR confirmed the upregulation of the well-established downstream targets of FOXO TF, *CDKN1B* and *BIM*,[7] after TAS-117 treatment (Figure 5B and Figure S4B). We focused on FOXO3 as it was the main *FOXO* family gene expressed in MM cells according to our RNA-seq data, besides its role in MM therapy.[41] Akt phosphorylates FOXO3, thereby excluding it to the cytoplasm, and, hence, restricts its transcriptional activity.[7] We examined the nuclear localization of FOXO3 following TAS-117 treatment by immunostaining, and found that TAS-117 significantly enhanced the nuclear accumulation of FOXO3 in MM.1S and H929 cell lines, as depicted by both the immunostaining images (Figure 5C and Figure S4C) and the digital calculations of the nuclear subset of FOXO3 in the TAS-117-treated group versus the untreated control (Figure 5D). FOXO3 regulates its own promoter.[42] Indeed, *FOXO3* and *FOXO4* were also upregulated after TAS-117 treatment (Figure 5B and Figure S4B).

In four different murine studies that analyzed the binding sites of Foxo TF,[43] 461 common genes, including the *Ezh1* promoter, were identified to have prominent Foxo peaks, in neuronal progenitors,[44] Tregulatory cells,[45] CD8$^+$ cells[46] and pre–B cells,[47] suggesting that Foxo TF share some common target genes in different contexts. Based on this observation, we hypothesized that FOXO3 may be a regulatory partner for the human *EZH1* gene in myeloma cells in response to TAS-117 treatment. To this end, we analyzed Foxo-binding loci on the mouse *Ezh1* promoter in the previously mentioned studies. We found that they shared similar Foxo-binding peaks spanning approximately 160 bp upstream to 300 bp downstream of the *Ezh1* transcription start site (TSS) (Figure S4D). FOXO TF are characterized by their conserved DNA-binding domain,[7] and more than 80% of FOXO3-binding sites share the common consensus binding motif GTAAACAA.[48] Interestingly, this binding motif was found both in human *EZH1* (+48 from the TSS) and mouse *Ezh1* (+77 from the TSS) promoter regions corresponding to the Foxo peaks observed in the murine studies data (Figure S4E). We designed two primers for the human *EZH1* promoter to investigate whether FOXO TF regulates *EZH1* promoter in response to TAS-117 treatment (Figure 5E). We then performed ChIP followed by quantitative PCR on TAS-117-treated and TAS-117-untreated cells. TAS-117 promoted the binding of FOXO3 to the *EZH1* promoter, in addition to one of the canonical FOXO3 targets, the *BIM* promoter, in MM.1S and H929 cells (Figure 5F). To further confirm our results, we expressed shRNA against *FOXO3*, *shFOXO3* and control, *shScramble*, in H929 cells using lentiviral vectors. The knockdown of *FOXO3* induced the downregulation of *EZH1* mRNA
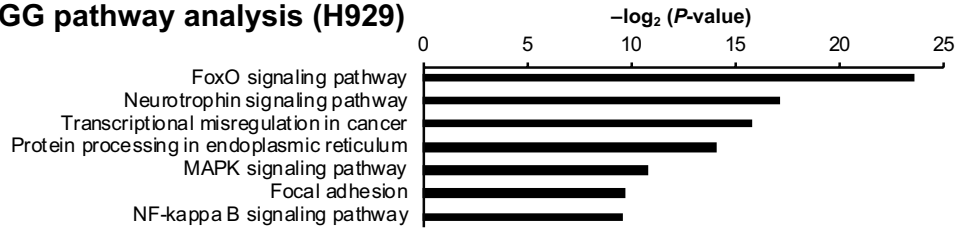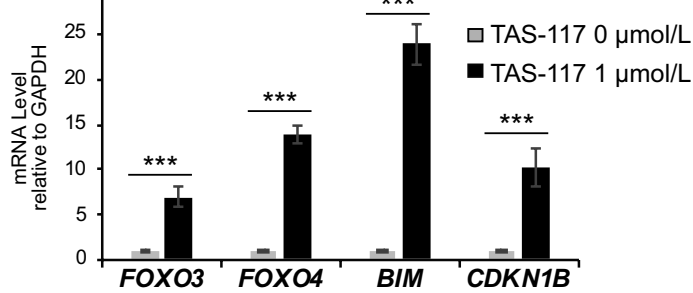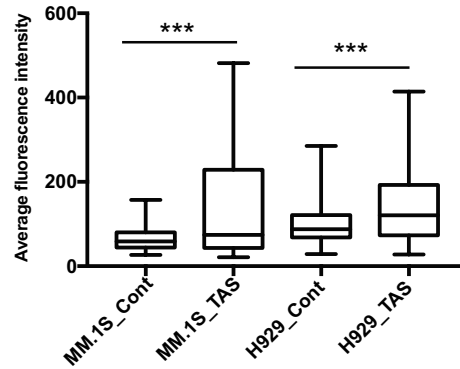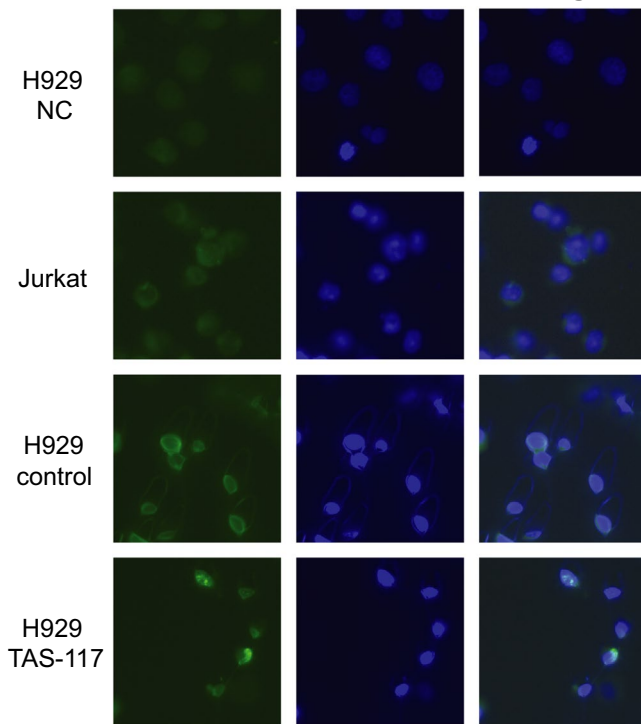
in addition to *CDKN1B*, as a common target of FOXO3 (Figure 5G). Moreover, as reported in primary hematopoietic cells,[49] *FOXO3* knockdown attenuated the growth of MM cells (Figure S4F). Collectively, these results provide a regulatory mechanism for the activation of *EZH1* transcription after Akt inhibition, which was mediated by FOXO3 TF.
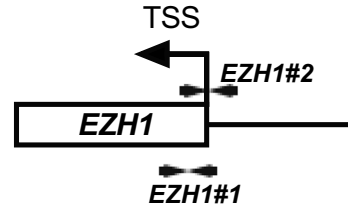
4 | DISCUSSION

We herein investigated the molecular interactions between the PI3K/Akt cascade and the catalytic components of PRC2, EZH2 and EZH1, and demonstrated that a "dual" EZH2/EZH1 inhibitor, UNC1999, but not "selective" EZH2 inhibitor GSK126, exerted synergistic anti–myeloma effects when combined with the Akt inhibitor, TAS-117. This combination has potential as a therapeutic option for a broad range of myeloma patients because in addition to the basal activation of Akt in myeloma cells, not only the interaction with bone marrow stromal cells but also the response to the conventional anti–myeloma therapy, namely, proteasome inhibitors, results in the further activation of Akt.[10]

Several TF have been reported to bind and regulate the *EZH2* promoter, including MAPK/PI3K pathways through their downstream Elk1[22] or activator protein 1 (AP-1),[24] KRAS mutations via ERK or Akt,[23] and NF-κB.[14] We previously demonstrated that E2F1 activity was closely associated with the downregulation of *EZH2* in MM in response to bortezomib treatment.[19] E2F is inactivated through the formation of an inactive complex with Rb. In contrast, Akt activates cyclins and cyclin-dependent kinases (CDK), which, in turn, hyper-phosphorylate Rb, thereby inducing the release and activation of E2F.[50] In the present study, TAS-117 induced the upregulation of *CDKN1B*, through FOXO upregulation,[7] in addition to the inactivation of cyclins and CDK and, hence, hypo-phosphorylated Rb, thereby stabilizing the Rb-E2F1 complex and diminishing free E2F1 available for binding to its target genes, including its own promoter[51] and the *EZH2* promoter.[19,36,37]
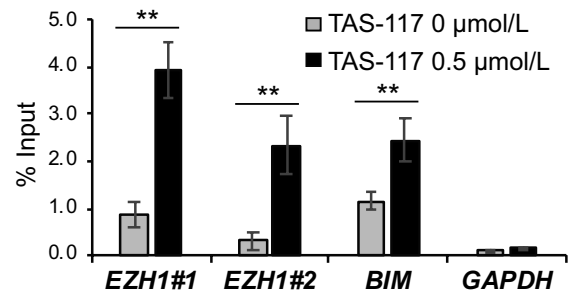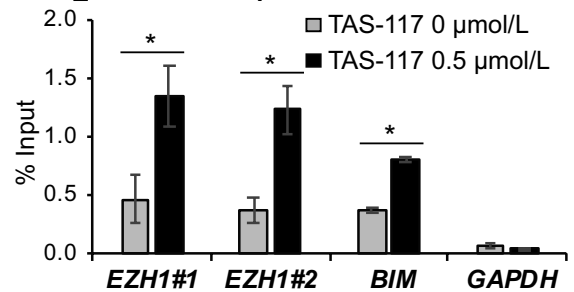
In contrast to these insights into *EZH2* transcriptional regulation, the transcriptional regulation of *EZH1* has not yet been fully clarified. Extensive ChIP-seq analyses of FOXO TF-binding targets[43] revealed that a significant number of genes, including the *Ezh1* promoter, were "core-bound" by Foxo1 and Foxo3 in four different murine studies.[43-47] Akt phosphorylates FOXO3 and promotes its nuclear exit,[7] thereby diminishing its transcriptional activity, including its own regulation.[42] Consistent with these findings, we found that TAS-117 enhanced FOXO3 nuclear accumulation in myeloma cells and, interestingly, increased the binding of FOXO3 to the *EZH1* promoter, thereby controlling *EZH1* compensatory upregulation. To the best of our knowledge, this is the first study to show a regulatory mechanism for *EZH1* transcription in MM. Collectively, the present study supports the theory that histone modifications are part of conventional signaling cascades under context-dependent control. Based on the present results, we propose *EZH2* and *EZH1* as eventual components of the PI3K/Akt pathway and E2F1 and FOXO3 as intermediate nuclear

(A) KEGG pathway analysis (H929)

FoxO signaling pathway
Neurotrophin signaling pathway
Transcriptional misregulation in cancer
Protein processing in endoplasmic reticulum
MAPK signaling pathway
Focal adhesion
NF-kappa B signaling pathway

$-\log_2$ (P-value)

(B) H929

mRNA Level relative to GAPDH

☐ TAS-117 0 µmol/L
■ TAS-117 1 µmol/L

FOXO3 FOXO4 BIM CDKN1B
*** *** *** ***

(C)

FOXO3 ab   DAPI   Merge

H929 NC

Jurkat

H929 control

H929 TAS-117

(D) FOXO3 nuclear fraction

Average fluorescence intensity

MM.1S_Cont MM.1S_TAS H929_Cont H929_TAS
*** ***

(E)

TSS

EZH1#2

EZH1

EZH1#1

(F) MM.1S_FOXO3 ChIP-qPCR

% Input

☐ TAS-117 0 µmol/L
■ TAS-117 0.5 µmol/L

EZH1#1 EZH1#2 BIM GAPDH
** ** **

H929_FOXO3 ChIP-qPCR

% Input

☐ TAS-117 0 µmol/L
■ TAS-117 0.5 µmol/L

EZH1#1 EZH1#2 BIM GAPDH
* * *

(G) H929

mRNA Level relative to GAPDH

☐ shScramble
■ shFOXO3

FOXO3 EZH1 CDKN1B
*** * *

FIGURE 5 FOXO3 regulates the *EZH1* promoter in response to the TAS-117 treatment. A, Gene ontology analysis (KEGG pathway) of the enriched gene list in H929 cells (>1.5-fold) after the treatment with TAS-117 (0.5 μmol/L) for 24 h, using DAVID Bioinformatics Resources. Bars represent −log$_2$ of *P*-values for the corresponding pathway. B, Quantitative RT-PCR analysis for *FOXO3*, *FOXO4*, *BIM* and *CDKN1B* mRNA expression in H929 cells treated with TAS-117 (1 μmol/L) for 24 h. The *y*-axis represents fold changes after the normalization to *GAPDH*, and error bars represent the SD of triplicates. Significance was indicated relative to the untreated control. C, Immunofluorescence staining of the anti–FOXO3 antibody in H929 cells treated with or without TAS-117 at 0.5 μmol/L for 24 h, using Jurkat cells as a positive control. H929 cells lacking the primary antibody treatment were used as a negative control (NC). D, Digital representation of the average fluorescence intensity of the FOXO3 nuclear fraction in MM.1S and H929 cells treated with or without TAS-117 at 0.5 μmol/L for 24 h. Significance is indicated relative to the untreated control. E, Schematic representation of the location of the primer sets for the human *EZH1* promoter region. F, ChIP-qPCR analysis for FOXO3 occupancy on the *EZH1* promoter in MM.1S "upper" and H929 "lower" cells treated with or without 0.5 μmol/L of TAS-117 for 24 h. *BIM* and *GAPDH* promoters were used as positive and negative controls, respectively. Values correspond to the mean percentage of the input enrichment ± SD of triplicate qPCR reactions. Primer sequences for *EZH1*, *BIM* and *GAPDH* promoters are available in Table S2. Significance is indicated relative to the untreated control. G, Quantitative RT-PCR analysis for *FOXO3* and *EZH1* mRNA expression in H929 cells transduced with shRNA lentiviral vectors against *FOXO3* (*shFOXO3*) and control (*shScramble*) *CDKN1B* was used as the positive target for FOXO3. The *y*-axis represents fold changes after the normalization to *GAPDH*, and error bars represent the SD of triplicates. Significance is indicated relative to *shScramble*. *$P < 0.05$; **$P < 0.01$; ***$P < 0.001$ by Student's *t* test, except D, for which Welch's test was used

effectors with the ability to regulate *EZH2* and *EZH1* transcription, respectively.

Despite the development of selective EZH2 inhibitors in clinical trials, it is clear that the inhibition of EZH2 alone is insufficient for the complete disruption of PRC2 oncogenic functions.[19-21] Although inconsequential to EZH2 functions, EZH1 can augment and maintain PRC2 activities.[17,18,39] We herein clearly demonstrated that EZH1 contributes to an important compensatory mechanism in MM. While *EZH2* was abrogated after TAS-117 treatment, *EZH1* was markedly upregulated with the retention of H3K27me3. Therefore, the combination with dual EZH2/EZH1 inhibition using UNC1999 was more effective than with selective EZH2 inhibition using GSK126. We previously reported that the combination of bortezomib with UNC1999 exerted superior cytotoxic effects to that with GSK126 against PRC2-dependent cancers, MM and prostate cancer.[19] EZH1 has an undeniable role in the maintenance of cancer-initiating cells. Nakagawa and colleagues recently clarified the intimate role of EZH1 in addition to EZH2 in the maintenance of myeloma stem cells,[20] proposing that the inhibition of both EZH2 and EZH1 is crucial for the eradication of myeloma stem cells. This was further supported by the evidence showing that the deletion of both *Ezh1* and *Ezh2* had more significant effects than the deletion of *Ezh2* alone in eradicating quiescent leukemia stem cells.[21] These findings and the present results emphasize the crucial role of the inhibition of EZH1 as well as EZH2 for effective cancer treatment and that a significant portion of myeloma patients will benefit from the combination of TAS-117 with dual EZH2/EZH1 inhibition.

The responsiveness of myeloma cells to Akt inhibition is linked to the basal level of Akt activation.[10,29] We herein showed that TAS-117 sensitivity was not only associated with high p-Akt levels but also with low/deleted *PTEN* levels, and cells with high *PTEN* levels were more resistant to Akt inhibition. Furthermore, MAPK activation constitutes an apparent intrinsic resistance mechanism to Akt inhibition in MM.[10,29,30] Dynamic crosstalk between the PI3K/Akt and MEK/ERK pathways may eventually play a role in modulating the resistance of MM cells to the inhibition of a single pathway. Either pathway can regulate the

other through several overlapping inhibitory feedback mechanisms; relieving one feedback may secondarily activate the other pathway.[52] One of the most important downstream targets of Akt is mTORC1. The phosphorylation of mTORC1 inhibits S6K/IRS1 axis and triggers a brake on PI3K activity, thereby negatively regulating Akt activity. The inhibition of Akt/mTORC1 relieves this feedback and activates PI3K,[53] which, in turn, activates RAS and then feeds into the activation of MEK/ERK cascade.[54] In contrast, Akt inhibition-mediated FOXO pathway activation promotes FOXO-driven transcription of several receptor tyrosine kinases, leading to stronger PI3K/MEK/ERK activation.[52] In the present study, we observed the activation of MAPK, depicted by increases in p-ERK1/2 levels, after TAS-117 treatment, which was similarly reported in MM using different allosteric Akt inhibitors,[10,29,30] with the concurrent phosphorylation of PI3K regulatory subunit p85, and, hence, PI3K activation. Notably, UNC1999, a dual EZH1/2 inhibitor, overcame the effects of these resistance-inducing pathways in Akt inhibition (data not shown), supporting its potential as a companion drug of Akt inhibitors.

In conclusion, the present results defined novel signaling-epigenetic crosstalk between the PI3K/Akt pathway and the PRC2 components, EZH2 and EZH1, and demonstrated that Akt inhibition modulates *EZH2* and *EZH1* levels via the Akt downstream effectors E2F1 and FOXO3, respectively. Therefore, targeting both EZH2 and EZH1 in addition to Akt inhibition may be a promising means to eradicate MM, leading to significant advances in treatment.

DISCLOSURE

The authors have no competing financial interests to declare.

ORCID

Mohamed Rizk https://orcid.org/0000-0002-1059-1524

REFERENCES

1. Mimura N, Hideshima T, Anderson KC. Novel therapeutic strategies for multiple myeloma. *Exp Hematol.* 2015;43:732-41.
2. Ramakrishnan V, Kumar S. PI3K/AKT/mTOR pathway in multiple myeloma: from basic biology to clinical promise. *Leuk Lymphoma.* 2018;59:2524-2534.
3. Hideshima T, Nakamura N, Chauhan D, Anderson KC. Biologic sequelae of interleukin-6 induced PI3-K/Akt signaling in multiple myeloma. *Oncogene.* 2001;20:5991-6000.
4. Hideshima T, Mitsiades C, Tonon G, Richardson PG, Anderson KC. Understanding multiple myeloma pathogenesis in the bone marrow to identify new therapeutic targets. *Nat Rev Cancer.* 2007;7:585-598.
5. Chang H, Qi XY, Claudio J, Zhuang L, Patterson B, Stewart AK. Analysis of PTEN deletions and mutations in multiple myeloma. *Leuk Res.* 2006;30:262-265.
6. Ismail SI, Mahmoud IS, Msallam MM, Sughayer MA. Hotspot mutations of PIK3CA and AKT1 genes are absent in multiple myeloma. *Leuk Res.* 2010;34:824-826.
7. Zhang X, Tang N, Hadden TJ, Rishi AK. Akt, FoxO and regulation of apoptosis. *Biochim Biophys Acta.* 2011;11:31.
8. Konopleva MY, Walter RB, Faderl SH, et al. Preclinical and early clinical evaluation of the oral AKT inhibitor, MK-2206, for the treatment of acute myelogenous leukemia. *Clin Cancer Res.* 2014;20:2226-2235.
9. Nitulescu GM, Margina D, Juzenas P, et al. Akt inhibitors in cancer treatment: the long journey from drug discovery to clinical use (Review). *Int J Oncol.* 2016;48:869-885.
10. Mimura N, Hideshima T, Shimomura T, et al. Selective and potent Akt inhibition triggers anti-myeloma activities and enhances fatal endoplasmic reticulum stress induced by proteasome inhibition. *Cancer Res.* 2014;74:4458-4469.
11. Iwama A. Polycomb repressive complexes in hematological malignancies. *Blood.* 2017;130:23-29.
12. Yamagishi M, Uchimaru K. Targeting EZH2 in cancer therapy. *Curr Opin Oncol.* 2017;29:375-381.
13. Croonquist PA, Van Ness B. The polycomb group protein enhancer of zeste homolog 2 (EZH 2) is an oncogene that influences myeloma cell growth and the mutant ras phenotype. *Oncogene.* 2005;24:6269-6280.
14. Fujikawa D, Nakagawa S, Hori M, et al. Polycomb-dependent epigenetic landscape in adult T-cell leukemia. *Blood.* 2016;127:1790-1802.
15. Kalushkova A, Fryknäs M, Lemaire M, et al. Polycomb target genes are silenced in multiple myeloma. *PLoS ONE.* 2010;5:e11483.
16. Pawlyn C, Bright MD, Buros AF, et al. Overexpression of EZH2 in multiple myeloma is associated with poor prognosis and dysregulation of cell cycle control. *Blood Cancer J.* 2017;7:e549.

17. Margueron R, Li G, Sarma K, et al. Ezh1 and Ezh2 maintain repressive chromatin through different mechanisms. *Mol Cell.* 2008;32:503-518.
18. Mochizuki-Kashio M, Aoyama K, Sashida G, et al. Ezh2 loss in hematopoietic stem cells predisposes mice to develop heterogeneous malignancies in an Ezh1-dependent manner. *Blood.* 2015;126:1172-1183.
19. Rizq O, Mimura N, Oshima M, et al. Dual inhibition of EZH2 and EZH1 sensitizes PRC2-dependent tumors to proteasome inhibition. *Clin Cancer Res.* 2017;23:4817-4830.
20. Nakagawa M, Fujita S, Katsumoto T, et al. Dual inhibition of enhancer of zeste homolog 1/2 overactivates WNT signaling to deplete cancer stem cells in multiple myeloma. *Cancer Sci.* 2018;21:13840.
21. Fujita S, Honma D, Adachi N, et al. Dual inhibition of EZH1/2 breaks the quiescence of leukemia stem cells in acute myeloid leukemia. *Leukemia.* 2018;32:855-864.
22. Fujii S, Tokita K, Wada N, et al. MEK-ERK pathway regulates EZH2 overexpression in association with aggressive breast cancer subtypes. *Oncogene.* 2011;30:4118-4128.
23. Riquelme E, Behrens C, Lin HY, et al. Modulation of EZH2 Expression by MEK-ERK or PI3K-AKT signaling in lung cancer is dictated by different KRAS oncogene mutations. *Cancer Res.* 2016;76:675-685.
24. Ferraro A, Mourtzoukou D, Kosmidou V, et al. EZH2 is regulated by ERK/AKT and targets integrin alpha2 gene to control epithelial-mesenchymal transition and anoikis in colon cancer cells. *Int J Biochem Cell Biol.* 2013;45:243-254.
25. Konze KD, Ma A, Li F, et al. An orally bioavailable chemical probe of the lysine methyltransferases EZH2 and EZH1. *ACS Chem Biol.* 2013;8:1324-1334.
26. Wildey GM, Howe PH. Runx1 is a co-activator with FOXO3 to mediate transforming growth factor beta (TGFbeta)-induced Bim transcription in hepatic cells. *J Biol Chem.* 2009;284:20227-20239.
27. Eijkelenboom A, Mokry M, de Wit E, et al. Genome-wide analysis of FOXO3 mediated transcription regulation through RNA polymerase II profiling. *Mol Syst Biol.* 2013;9:638.
28. Chou TC, Talalay P. Quantitative analysis of dose-effect relationships: the combined effects of multiple drugs or enzyme inhibitors. *Adv Enzyme Regul.* 1984;22:27-55.
29. Ramakrishnan V, Kimlinger T, Haug J, et al. Anti-myeloma activity of Akt inhibition is linked to the activation status of PI3K/Akt and MEK/ERK pathway. *PLoS ONE.* 2012;7:e50005.
30. Hideshima T, Catley L, Yasui H, et al. Perifosine, an oral bioactive novel alkylphospholipid, inhibits Akt and induces in vitro and in vivo cytotoxicity in human multiple myeloma cells. *Blood.* 2006;107:4053-4062.
31. Ri M, Iida S, Nakashima T, et al. Bortezomib-resistant myeloma cell lines: a role for mutated PSMB5 in preventing the accumulation of unfolded proteins and fatal ER stress. *Leukemia.* 2010;24:1506-1512.
32. Bisserier M, Wajapeyee N. Mechanisms of resistance to EZH2 inhibitors in diffuse large B-cell lymphomas. *Blood.* 2018;131:2125-2137.
33. Xu B, On DM, Ma A, et al. Selective inhibition of EZH2 and EZH1 enzymatic activity by a small molecule suppresses MLL-rearranged leukemia. *Blood.* 2015;125:346-357.
34. McCabe MT, Ott HM, Ganji G, et al. EZH2 inhibition as a therapeutic strategy for lymphoma with EZH2-activating mutations. *Nature.* 2012;492:108-112.
35. Chou TC. Theoretical basis, experimental design, and computerized simulation of synergism and antagonism in drug combination studies. *Pharmacol Rev.* 2006;58:621-681.
36. Bracken AP, Pasini D, Capra M, Prosperini E, Colli E, Helin K. EZH2 is downstream of the pRB-E2F pathway, essential for proliferation and amplified in cancer. *Embo J.* 2003;22:5323-5335.
37. Lee S-R, Roh Y-G, Kim S-K, et al. Activation of EZH2 and SUZ12 regulated by E2F1 predicts the disease progression and aggressive characteristics of bladder cancer. *Clin Cancer Res.* 2015;21:5391-5403.

38. Brennan P, Babbage JW, Burgering BM, Groner B, Reif K, Cantrell DA. Phosphatidylinositol 3-kinase couples the interleukin-2 receptor to the cell cycle regulator E2F. *Immunity.* 1997;7:679-689.

39. Aoyama K, Oshima M, Koide S, et al. Ezh1 targets bivalent genes to maintain self-renewing stem cells in Ezh2-insufficient myelodysplastic syndrome. *iScience.* 2018;9:161-174.

40. da Huang W, Sherman BT, Lempicki RA. Systematic and integrative analysis of large gene lists using DAVID bioinformatics resources. *Nat Protoc.* 2009;4:44-57.

41. Zhou Y, Uddin S, Zimmerman T, Kang JA, Ulaszek J, Wickrema A. Growth control of multiple myeloma cells through inhibition of glycogen synthase kinase-3. *Leuk Lymphoma.* 2008;49:1945-1953.

42. Lützner N, Kalbacher H, Krones-Herzig A, Rösl F. FOXO3 is a glucocorticoid receptor target and regulates LKB1 and its own expression based on cellular AMP levels via a positive autoregulatory loop. *PLoS ONE.* 2012;7:e42166.

43. Webb AE, Kundaje A, Brunet A. Characterization of the direct targets of FOXO transcription factors throughout evolution. *Aging Cell.* 2016;15:673-685.

44. Webb A, Pollina E, Vierbuchen T, et al. FOXO3 shares common targets with ASCL1 genome-wide and inhibits ASCL1-dependent neurogenesis. *Cell Rep.* 2013;4:477-491.

45. Ouyang W, Liao W, Luo CT, et al. Novel Foxo1-dependent transcriptional programs control T(reg) cell function. *Nature.* 2012;491:554-559.

46. Kim MV, Ouyang W, Liao W, Zhang MQ, Li MO. The transcription factor Foxo1 controls central-memory CD8+ T cell responses to infection. *Immunity.* 2013;39:286-297.

47. Ochiai K, Maienschein-Cline M, Mandal M, et al. A self-reinforcing regulatory network triggered by limiting IL-7 activates pre-BCR signaling and differentiation. *Nat Immunol.* 2012;13:300-307.

48. Chen X, Ji Z, Webber A, Sharrocks AD. Genome-wide binding studies reveal DNA binding specificity mechanisms and functional interplay amongst Forkhead transcription factors. *Nucleic Acids Res.* 2016;44:1566-1578.

49. Tothova Z, Kollipara R, Huntly BJ, et al. FoxOs are critical mediators of hematopoietic stem cell resistance to physiologic oxidative stress. *Cell.* 2007;128:325-339.

50. Nevins JR. The Rb/E2F pathway and cancer. *Hum Mol Genet.* 2001;10:699-703.

51. Araki K, Nakajima Y, Eto K, Ikeda MA. Distinct recruitment of E2F family members to specific E2F-binding sites mediates activation and repression of the E2F1 promoter. *Oncogene.* 2003;22:7632-7641.

52. Chandarlapaty S, Sawai A, Scaltriti M, et al. AKT inhibition relieves feedback suppression of receptor tyrosine kinase expression and activity. *Cancer Cell.* 2011;19:58-71.

53. O'Reilly KE, Rojo F, She Q-B, et al. mTOR inhibition induces upstream receptor tyrosine kinase signaling and activates Akt. *Cancer Res.* 2006;66:1500-1508.

54. Carracedo A, Ma L, Teruya-Feldstein J, et al. Inhibition of mTORC1 leads to MAPK pathway activation through a PI3K-dependent feedback loop in human cancer. *J Clin Invest.* 2008;118:3065-3074.

SUPPORTING INFORMATION

Additional supporting information may be found online in the Supporting Information section.